

Analysis of typhoon rananim using ATOVS retrieval products

Liu zhe

Institute of Meteorology, PLA University of Science and Technology, Nanjing, China

Han zhigang Zhao zengliang

Beijing Institute of Applied Meteorology, Beijing, China

Zhang fengying

National Satellite Meteorology Center, Beijing, China

Abstract The number 0414 typhoon rananim has caused serious damage to part of the districts in Zhejiang province of China. In this paper, the thermal structure of rananim was analyzed with the products of temperature and humidity profiles retrieved from ATOVS, which can receive the microwave radiation through the cirrus clouds above typhoon and detect the temperature anomalies of it. Under hydrostatic and gradient balance assumption, using NCEP reanalyzed data as initial parameter and four sets of ATOVS data mapped with rananim, the minimum sea level pressure (MSLP) and maximum wind speed (MSW) were also calculated respectively and compared with the typhoon warning report of Central Meteorological Station (CMS) estimated from the visible and infrared method, the mean discrepancy of MSLP and MSW is found to be 11.8hPa and 4.3m/s respectively, showing similar time-variant tendency of rananim as described by CMS. What's more, it can depict the three-dimensional structure of tangential wind fields too.

Introduction

Since the mid-1960s in 20th century, extensive research has examined tropical cyclone intensity estimation using meteorological satellite. Nowadays, the most widely used tropical cyclone estimation and position analysis techniques employed by operational forecasters was by analyzing the infrared and visible satellite imagery (Dvorak 1984, Velden and Olander 1998). That technique uses information gleaned from a storm's cloud pattern and the day-to-day changes in that pattern in visible imagery to assess the stage of development of a tropical cyclone. While these products provide invaluable information about the overall structure and strength of a tropical system, they often can't penetrate clouds to ascertain low-level storm structure. Because of the shortcomings of estimating tropical cyclone intensity, an alternate method is desired that is entirely objective and is applicable to tropical cyclone. Certain wavelengths of microwave energy are able to penetrate ice clouds (such as the cirrus above the storm). What's more, except in heavily precipitating areas, microwaves are unaffected by hydrometeor contamination. Therefore, it offers a unique perspective into tropical cyclone structure.

Kidder et al (1978) first attempted passive microwave in monitoring tropical cyclone intensity estimation using the Scanning Microwave Spectrometer (SCAMS) aboard Nimbus-5 and Nimbus-6 satellites. Unfortunately, the extremely coarse horizontal resolution severely limited the ability of the sensor to sufficiently resolve the warm core. Velden and Smith (1983)

using the Microwave Sounding Unit (MSU) data to estimate the intensity and central pressure, which were flown aboard NOAA-6-14 satellites. They derived a set of linear regression coefficients that related observed brightness temperature anomalies with aircraft observed minimum sea level pressure.

The first Advanced Microwave Sounding Unit (AMSU) was launched aboard the NOAA-15 satellite on 13 May 1998. Kidder et al (2000) using the retrieved data from AMSU analyzed the upper tropospheric thermal anomalies; they also calculated the gradient winds from the temperature field. Brueske (2001) developed a method to explicitly account for subsampling and diffraction effects.

AMSU and the High-resolution Infrared Radiation Sounder (HIRS/3), which was flown aboard NOAA-KLM satellites, were called Advanced TIROS Operational Vertical Sounding (ATOVS). By using the International ATOVS Processing Package (IAPP) by Cooperative Institute of Meteorological Satellite Studies (CIMSS) of the University of Wisconsin (UW), the ATOVS data can be finally translated into the retrieval products including the atmospheric temperature profile, moisture profile, atmospheric total ozone, and other parameters in both clear and cloudy atmospheres. The algorithm that retrieves these parameters contains four steps:

- (1) cloud detection and removal;
- (2) bias adjustment for ATOVS measurements;
- (3) regression retrieval processes;
- (4) a nonlinear iterative physical retrieval.

ATOVS temperature and dew-point soundings were retrieved at 42 vertical levels from 0.1 to 1000hPa at the grid locations shown in Fig. 1. The resolution of retrieval products is about 50km under the nadir. The root mean square (rms) differences between ATOVS retrieval temperature profiles and radiosonde observation profiles are less than 2k and 2.5k when under the clear and cloudy weather respectively. As to dew-point profiles, the rms error is about 3.0-6.0k.

Data

The number 0414 typhoon rananim originated from the north-west of Guam at about 0000UTC on 9 Aug, during the following three days, it became strengthen and strengthen till it landed on Wenlin, Zhejiang province of China at 1200UTC on 12 Aug. Besides the ATOVS retrieval data, we employed the central position data and strengthen information from the typhoon warning report of CMS, which was estimated from the visible and infrared method. The tropical cyclone position estimate at 3-hourly intervals from the CMS are interpolated to the time of the ATOVS retrieval data.

Although the cross-track-scanning ATOVS retrieval products swaths are about 2000km wide, the sample was limited to those cases in which the typhoon center fell near the center of ATOVS retrieval swaths. Seen from the coincident infrared image, we can see the size of central clouds of rananim is about $12^{\circ} \times 12^{\circ}$. Therefore, the domain was set as 600-km radius

near the central of swaths. If the typhoon center falls in the domain (see Fig.1 (a)), then the retrieval data is suit for our research relatively. Sometimes, the typhoon center falls at or near the limb of the swaths (see Fig.1 (b)), because the data resolution is about 100km and a large portion of the analysis domain with no data. Therefore, these cases are not suit for research.

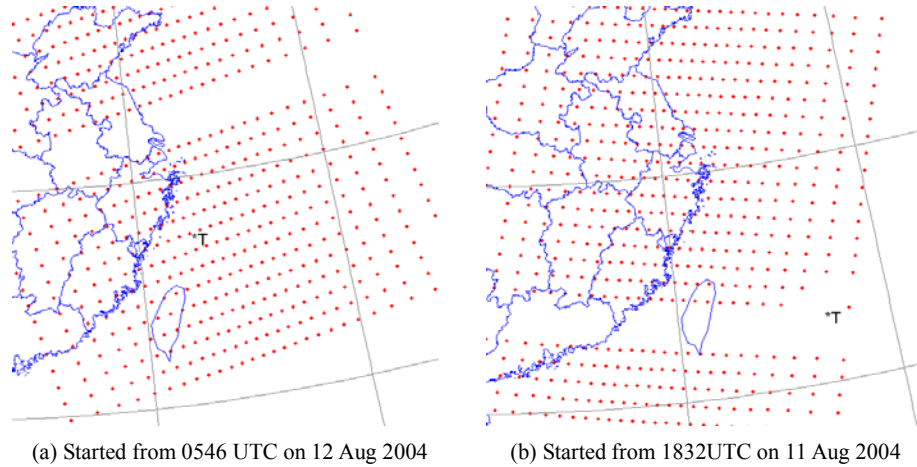


Fig. 1: A portion of the ATOVS retrieval products swath
(*T was the central position of typhoon rananim at that time)

Methods

First of all, we determine the domain of typhoon center cloud field according to the coincident infrared image, and then the temperature anomalies were calculated by subtracting the average temperature of outer radius from the temperature at each grid in the domain. By analyzing the cross-section of temperature anomalies, we can depict the warm-core lies in the upper-troposphere. By subtracting the dew-point temperature from the temperature of each grid, we can analysis the depression of dew point too, therefore, we can know more about the thermal structure about the typhoon rananim.

ATOVS retrieval temperatures at 23 levels from 920 to 50hPa were used to calculated the MSLP. Because of the high percentage of water vapor in the air near the typhoon eyewall, we should not neglect the effect of water vapor to the calculation of hydrostatic equation. In this paper, the virtual temperature effects were considered under the 500hPa pressure level. A two-pass distance-weighted analysis method (Barnes, 1964) was applied to interpolate the unevenly spaced temperature to a radial grid with the origin at the typhoon center. The surface temperature and pressure at the outer radius of the radial grid was obtained from the reanalysis for the NCEP global forecast model in time to ATOVS retrieval swaths. The hydrostatic equation was integrated at the outer radius of the domain up to the 50hPa level, after assuming the height of the 50hPa level was constant for all radii (Kidder, 2000). The hydrostatic equation was downward from 50 to 920hPa in the center grid. With the surface temperature afforded by NCEP analyzed data and the height of 920hPa level, the MSLP can be calculated finally.

Though surface pressure in tropical cyclones is nearly symmetric about the center, wind

speeds are notoriously asymmetric. Therefore, the distance-weighted analysis method was not applied to interpolate the unevenly spaced temperature. Assuming a linear variation in temperature with height between two pressure levels, the temperature and pressure as a function of height were calculated at any height from the surface to the tropopause. With the ideal gas equation, the density at each grid was calculated. Thus, we can use the radial pressure gradients to calculate the tangential wind of any height. In order to remove the cold anomalies caused by precipitation contamination, the negative temperature anomalies under 500hPa pressure levels were set to zero, and the tangential winds were recalculated. By comparing the two kinds of tangential wind fields, we can conclude the advantage and disadvantage of such method.

Results

Unfortunately, the area range of ATOVS data received by National Satellite Meteorology Center are not wide enough, which can only receive the data of part of the west-north Pacific besides the mainland from NOAA-16. By analyzing the area range of ATOVS retrieval data mapped with rananim typhoon tracks from CMS, we got four ideal sets of ATOVS retrieval data. In this text, we will discuss the characteristics of rananim from infrared image, microwave image, temperature anomalies image and the depression dew-point image, calculate the MSLP and MSW in each stage and compare with the typhoon warning report by CMS.

This set of ATOVS retrieval data we selected began at 0546UTC on 12 Aug, by interpolating the 3-hourly interval position and strength from the typhoon reporting, we got the central position of rananim at that time was (27.2°N, 122.6°E), the MSLP was 950hPa and the MWS near the eyewall was 45m/s. It showed that rananim belongs to mature stage. A portion of the ATOVS retrieval products swath was shown in Fig.1 (a) when the typhoon was closing to the swath center. Because of the relatively excellent resolution, it's well suit for research.

The much more frequent GOES-9 image is an indispensable tool for monitoring typhoon. As we can see from Fig.2 (a), rananim shows a well-developed broad central dense overcast (CDO) and a clear eye, several spiral bandings kept transporting water vapor from the warm sea to strengthen its intensity. Because microwave can penetrate certain kind of clouds, the AMSU provides views of structure inside tropical cyclone that are not observable with infrared sensors. The two AMSU-B window channels have the ability to sense precipitation-sized particles through the CDO. Relatively, the 150GHz window channel can depict the eye and the spiral bandings under the CDO more clearly because enhanced sensitivity to precipitation causes greater contrast between the eye and eyewall (Fig.2 (b)). We can also see from the microwave image that a gust from northeast has been enrolled in the outer cloud bands, with a stronger northeast trade wind, which will no doubt enhance the baroclinic instability of rananim and indicate it will be intensified in the future.

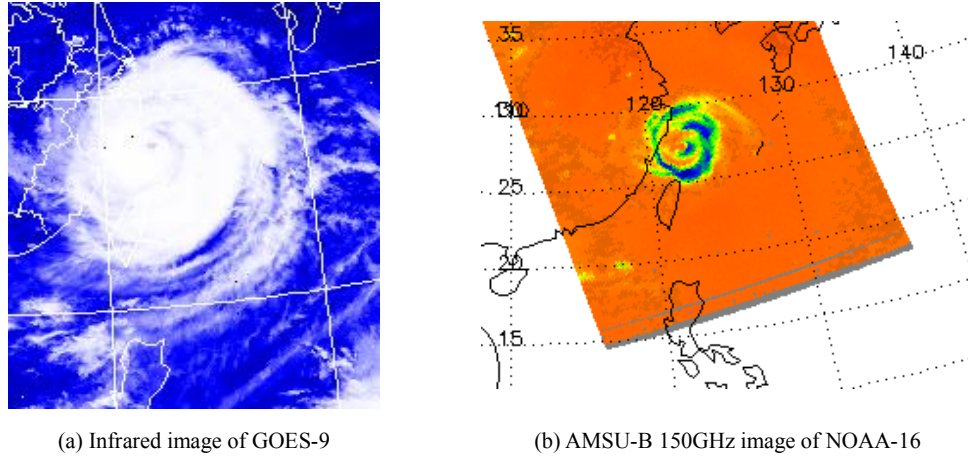
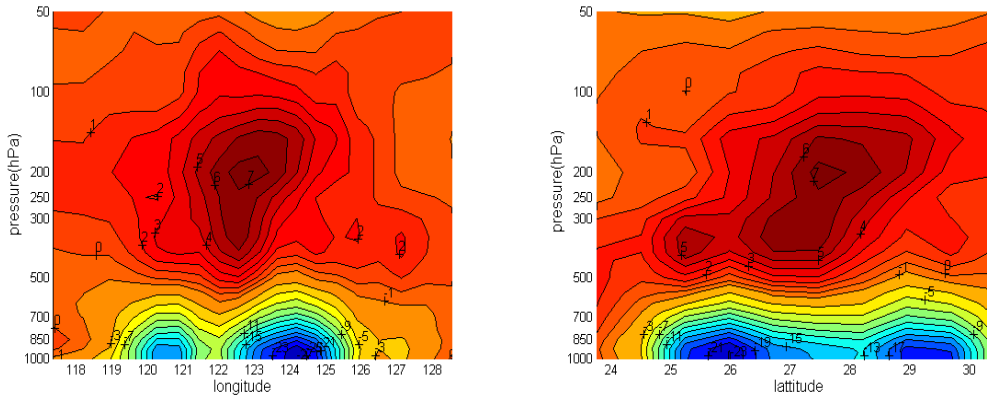


Fig.2: The coincident infrared and microwave image

Figure 3 shows the cross section of temperature anomalies along the latitude and longitude of the center position, we can see the structure of warm core clearly. During the development of typhoon, the relatively warm and moist inflow concentrates localized sensible heating in the eye and also contributes to additional heating throughout the column as the air ascends in the eyewall, and condensation ultimately results in the release of latent heat, which develops a warm core in the mid-upper of typhoon. We can see the maximum temperature anomaly is about 7k at 300hPa, the warm anomaly extending down into the lower troposphere at about 500hPa inside the eye. What's more, under 600hPa pressure level, there appear negative temperature anomalies, which were caused by heavy precipitation contamination. On the other hand, this contamination provides us useful information on the location and intensity of precipitation.



(a) Along the latitude of the central position of rananim (b) Along the longitude of the central position of rananim

Fig.3: The cross section of temperature anomalies

Figure 4 shows the cross section of the depression of dew point, we can see the air of lower troposphere near typhoon center is close to saturation; the vertical gradient of depression of dew point in the west of center is larger than the east, which means the instability structure of west is stronger and the air is more liable to be convection.

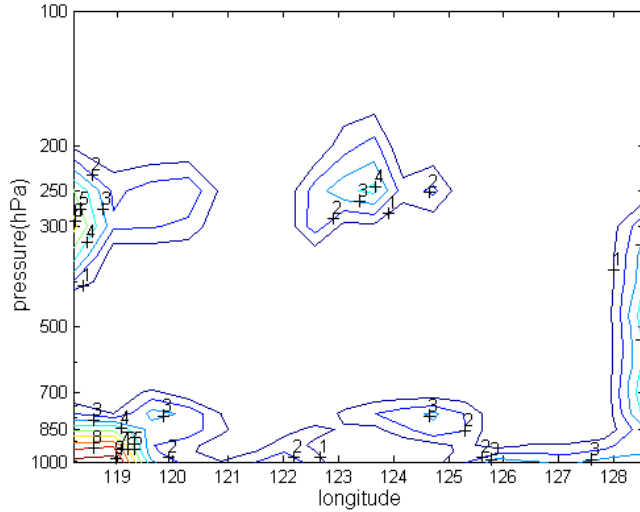


Fig.4: The cross section along the latitude of the depression of dew point

Figure 5(a) shows the tangential wind profile along the latitude of the center. With low-level cyclonic flow and an upper-level anticyclone, the basic structure of typhoon rananim's tangential wind field seems reasonable. The MSW is 52.3m/s at a radius of about 150km. However, the flow becomes anticyclonic in the low levels near the eyewall. This phenomenon is probably due to the unrealistic cold anomalies caused by the strong precipitation attenuation near the eyewall under 5km. According to the method introduced by kidder(2000), the temperature anomalies at pressure levels between the surface and 500hPa were set to zero and the gradient winds were recalculated. The result shows in figure 5(b). The tangential wind at large radius appears more reasonable. unfortunately, the MSW near the eyewall was down to 39m/s. This is because the corrected temperature can't replace the real temperature completely. Thus, other methods should be developed to address the precipitation attenuation problem.

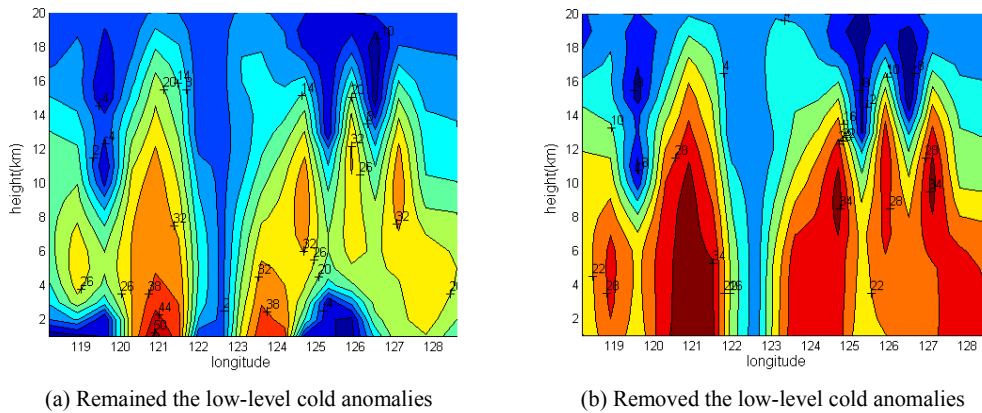


Fig.5: Tangential wind profile of rananim calculated from ATOVS data

Figure 6 shows the tangential wind fields at different altitude. The upper two charts are samples of lower level, apparently asymmetric. We can also see the precipitation attenuation near the typhoon eyewall. The other two charts are samples of higher level. Because typhoon is warm-core structure,

the radial pressure gradient grows small with height. To some exact height, the ascending air will flow outward, therefore, the flow becomes anticyclone in the high levels.

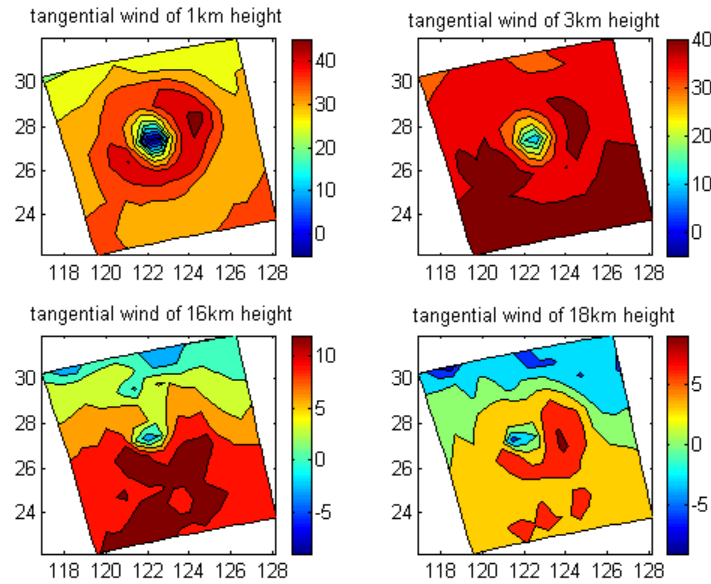


Fig.6: Tangential wind fields at different height calculated from ATVOS retrieval data

As figure 7 shows, the MSLP of the four sets of ATOVS data were calculated respectively and compared with the typhoon warning report of CMS, the mean discrepancy was 11.8hPa, showing similar time-variant tendency of rananim as described by CMS. Because warming in the upper troposphere is responsible for the surface pressure drop in the tropical cyclones, the maximum temperature anomaly has some correlation with MSLP.

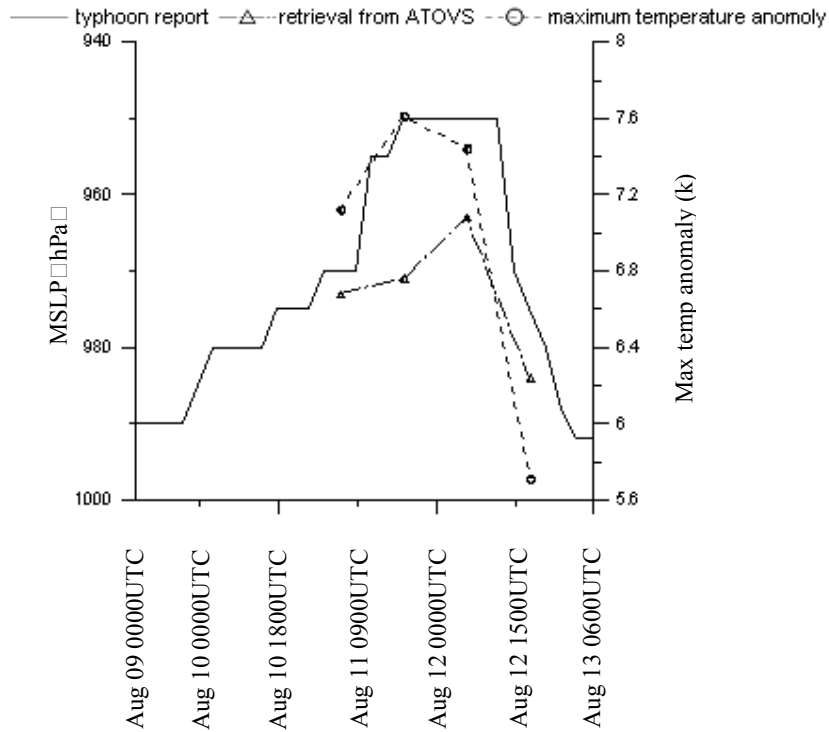


Fig. 7: Compared four sets of MSLP calculated from ATOVS with typhoon report

Shown as figure 8, the MWS was calculated from the ATOVS retrieval data. By comparing with the typhoon warning report of CMS, the mean discrepancy was found to be 4.3m/s, showing similar time-variant tendency. We found that there exist some correlation between the maximum temperature anomaly and MSW too.

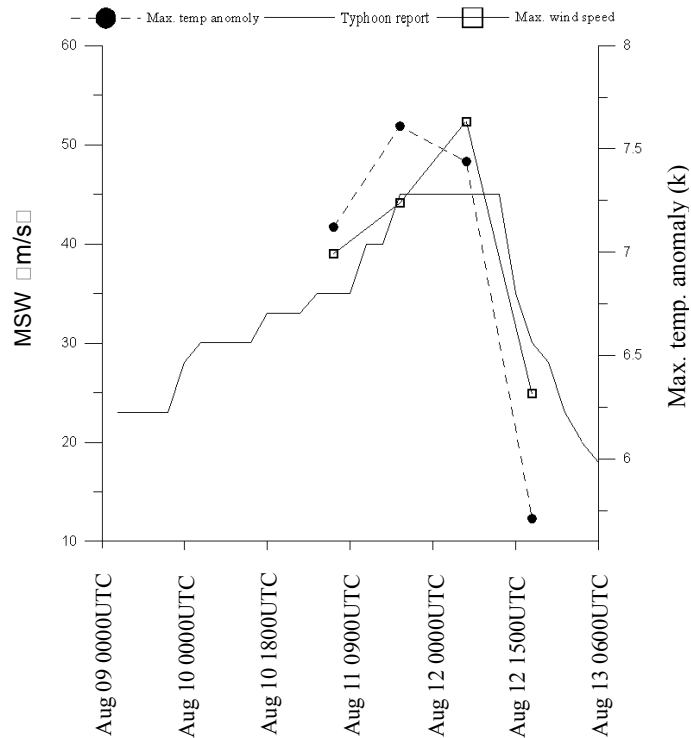


Fig.8: Compared four sets of MSW calculated from ATOVS with typhoon report

References

- Dvorak, 1984: Tropical cyclone intensity analysis using satellite data.. *NOAA Tech. Rep. NESDIS 11*, National Environmental Satellite Data Information Service, Washington, DC, 47pp
- Kidder, S. Q., W. M. Gray, and T. H. Vonder Haar, 1978: Estimating tropical cyclone central pressure and outer winds from satellite microwave data. *Mon. Wea. Rev.*, **106**, 1458-1464
- Velden, C. S., and W. L. Smith, 1983: Monitoring tropical cyclone evolution with NOAA satellite microwave observations. *J. Climate Appl. Meteor.*, **22**, 714-724
- Brueske, Kurt F., 2001: Satellite-based tropical cyclone intensity estimation using NOAA-KLM advanced microwave sounding unit (AMSU) data. PhD dissertation, 106 levels
- Kidder, S. Q., M. D. Goldberg, R. M. Zehr, M. DeMaria, J. F. W. Purdom, C. S. Velden, N. C. Grody, S. J. Kusselson, 2000: Satellite Analysis of Tropical Cyclones Using the Advanced Microwave Sounding Unit (AMSU). *Bull. Amer. Meteor. Soc.*, **81**(6), 1241-1260
- Li, Jun, Wolf. Thomas H, Global sounding of the atmosphere from ATOVS measurements: The algorithm and validation. *J. Appl. Meteor.* 2000, **39**: 1248-1268
- Barnes, S., 1964: A technique for maximizing details in numerical weather map analysis. *J. Appl. Meteor.*, **3**, 396-409
- Demuth, J. L. Evaluation of Advanced Microwave Sounding Unit Tropical-Cyclone Intensity and Size Estimation Algorithms. *J. Appl. Meteor.* 2004, **43**: 282-296

Proceedings of the Fourteenth International TOVS Study Conference

Beijing, China
25-31 May 2005

